Physics in Medicine & Biology

Dosimetric characterization of an encapsulated waterproof silicon carbide detector with UHDR electron and proton beams for FLASH radiotherapy

To cite this article: G Milluzzo *et al* 2025 *Phys. Med. Biol.* **70** 205019

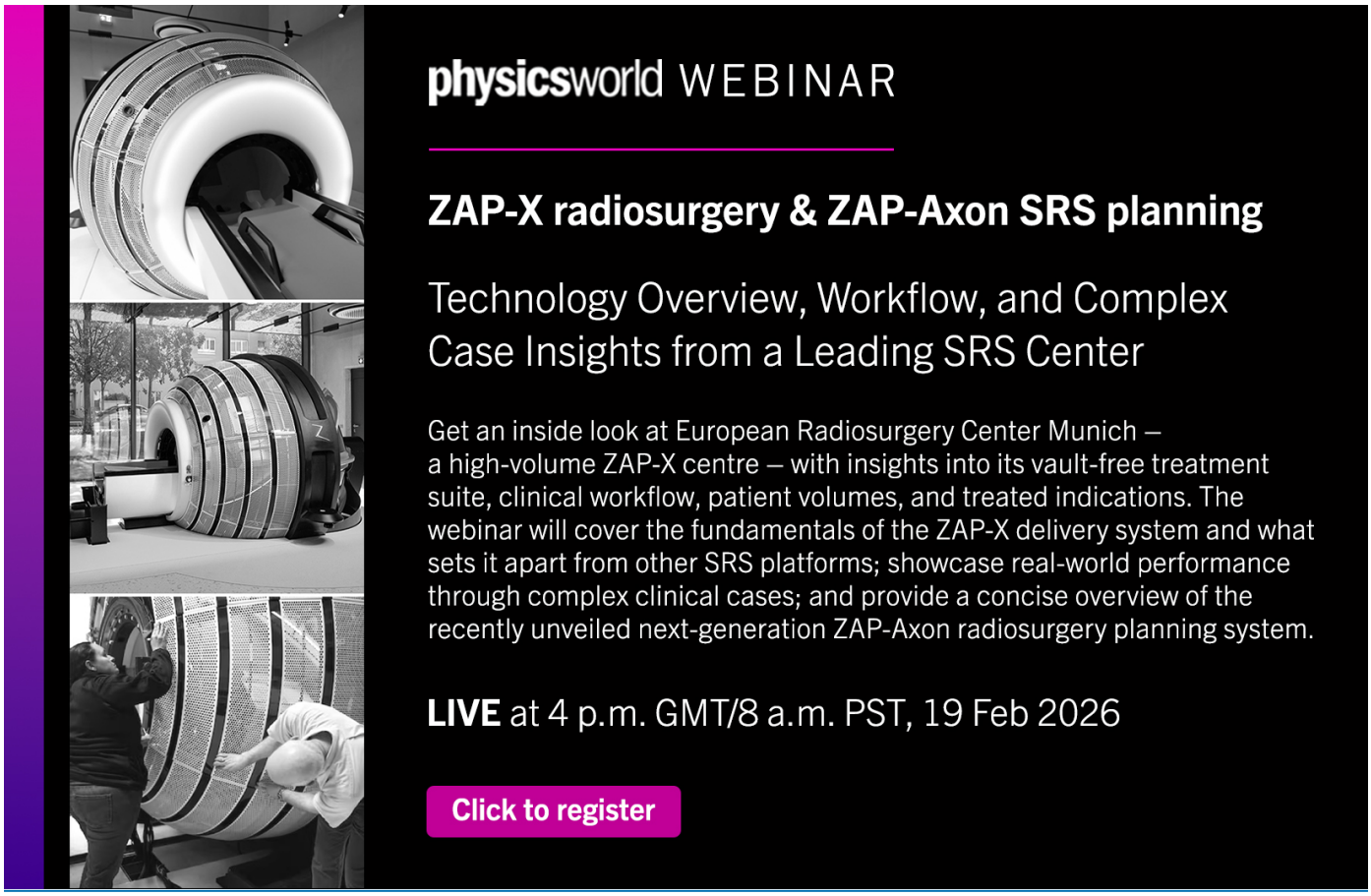

IOP Publishing Phys. Med. Biol. 70 (2025) 205019 https://doi.org/10.1088/1361-6560/ae0860

Physics in Medicine & Biology

IPEM Institute of Physics and Engineering in Medicine

PAPER

Dosimetric characterization of an encapsulated waterproof silicon carbide detector with UHDR electron and proton beams for FLASH radiotherapy

G Milluzzo[1,*], D Zitelli[1,2], A Cavalieri[3,4], M Celentano[4,5], F Di Martino[4,5,6], L Masturzo[4], C Okpuwe[1,7], J H Pensavalle[4], S Lorentini[8], E Scifoni[9,10], F Tommasino[9,10], A Trianni[8], G Trovato[1,7,11,12], E Verroi[9], A Quaranta[2,9], M Camarda[11] and F Romano[1]

[1] National Institute of Nuclear Physics (INFN), Catania Division, Via Santa Sofia, 64, Catania, Italy
[2] Department of Industrial Engineering, University of Trento, Via Sommarive 9, Povo, 38123 Trento, Italy
[3] Center for Instrument Sharing of the University of Pisa (CISUP), University of Pisa, Pisa, Italy
[4] Centro Pisano ricerca e implementazione clinica Flash Radiotherapy (CPFR@CISUP), Presidio S. Chiara, ed. 18 via Roma 67, Pisa, Italy
[5] National Institute of Nuclear Physics (INFN), Pisa Division, Largo B. Pontecorvo 3, Pisa, Italy
[6] Fisica Sanitaria, Azienda Ospedaliero Universitaria Pisa AOUP, ed.18 via Roma 67, Pisa, Italy
[7] Dipartimento di Fisica, Università degli Studi di Catania, Via Santa Sofia 64, Catania, Italy
[8] Medical Physics Department, Azienda Provinciale per i Servizi Sanitari (APSS), Trento, Italy
[9] INFN-TIFPA, Trento Institute for Fundamental Physics and Applications, Via Sommarive 14, Povo, 38123 Trento, Italy
[10] Department of Physics, University of Trento, Via Sommarive 14, Povo, 38123 Trento, Italy
[11] STLab srl, Via Anapo 53, 95126 Catania, Italy
[12] Istituto per la Microelettronica e Microsistemi CNR-IMM, Sezione di Catania, Strada VIII Zona Industriale 5, 95121 Catania, Italy
[*] Author to whom any correspondence should be addressed.

E-mail: giuliana.milluzzo@ct.infn.it

Keywords: FLASH radiotherapy, reference and relative dosimetry, silicon carbide, UHDR, electron and proton beams (Min.5-Max. 8)

OPEN ACCESS

RECEIVED
28 March 2025

REVISED
26 August 2025

ACCEPTED FOR PUBLICATION
17 September 2025

PUBLISHED
16 October 2025

Abstract

Silicon carbide (SiC) detectors have been widely demonstrated to be suitable alternative detectors for dosimetry in FLASH radiotherapy, showing radiation hardness and dose-rate independence at the FLASH radiotherapy instantaneous dose rates (IDRs). However, the practical use of such devices in the preclinical/clinical environment still requires the development of special handy housing enabling the quality assurance (QA) measurements under the reference dosimetric conditions. A 10 μm thick, 4.5 mm^2 area SiC detector produced by the STLab company was recently embedded at the INFN-Catania Division inside a plastic waterproof 15 mm diameter cylindrical housing. This encapsulated version of SiC (eSiC) allows the measurement of the dose in reference conditions and of the dose profiles in liquid/solid water phantoms for assuring high accuracy dosimetry QA procedures. Dosimetric characterizations were performed with both electron and proton beams at conventional and ultra-high dose rates (UHDR). A first experiment was carried out at the Centro Pisano for Flash Radiotherapy using UHDR 9 MeV electron beams to confirm the linearity of the charge response as a function of the dose per pulse after the encapsulation procedure. A linearity from 1.8 Gy/pulse up to about 12 Gy/pulse, corresponding to an IDR of 3 MGy s^{-1}, was found. The percentage depth dose (PDD) distribution in water of 9 MeV electron beams was also measured and compared with the PDD measured with a Freiburg Physikalisch-Technische Werkstätten Dr. Pychlau GmbH (PTW) flash diamond detector, used as reference dosimeter. The eSiC detector was also tested with proton beams accelerated by the IBA Proteus 235 cyclotron at the Trento Proton Therapy facility. A response independence on the total delivered dose (1–30 Gy) and average dose rate (50–530 Gy s^{-1}) was found using the UHDR 228 MeV proton beam available along the experimental beamline. The depth dose distribution measured with the eSiC within a liquid water phantom was successfully compared with the one simultaneously measured by the IBA PPC05 reference chamber, using 180 MeV clinical proton beams. The excellent results demonstrated that this first realized eSiC prototype can be used to

accurately perform reference and relative dosimetry with UHDR electron and proton beams, contributing to support the clinical translation of FLASH radiotherapy.

1. Introduction

In recent years, among the promising innovative radiotherapy (RT) techniques that are alternative to conventional one (CONV-RT), FLASH RT (FLASH-RT), based on the delivery of ultra-high dose rate (UHDR) particle beams (>40 Gy s^{-1}) in extremely short irradiation time (<300 ms), is emerging as it allows a significant reduction of the toxicities induced to the healthy tissues, while preserving the tumoral control in comparison with CONV-RT (Favaudon *et al* 2014, Vozenin *et al* 2019, Esplen *et al* 2020).

Thanks to the innovations in the field of accelerators (Di Martino *et al* 2020, 2023, Moeckli *et al* 2021, Schulte *et al* 2023), dosimetry (Romano *et al* 2022, Subiel and Romano 2023, Subiel *et al* 2024) and radiobiology (Montay-Gruel *et al* 2017, 2021, Vozenin *et al* 2024), clinical translation of FLASH-RT is rapidly progressing by means of trials using both electron and proton UHDR beams in domestic animals (Vozenin *et al* 2019, Konradsson *et al* 2021, Velalopoulou *et al* 2021, Rohrer Bley *et al* 2022, Børresen *et al* 2023) and clinical therapeutic trials on human patients, respectively using UHDR proton beams to treat bone metastases (FAST-01 trial NCT04592887) (Mascia *et al* 2023) and with low energy 9 MeV electron beams to treat skin cancer (IMPulse trial).

Nevertheless, one of the main challenges of FLASH-RT still relies on the accurate measurement of the delivered dose at these extreme dose rates as the traditional dosimeters recommended from the IAEA TRS-398 international protocol (Petersson *et al* 2017) for CONV-RT such as commercial ionization chambers, face remarkable charge recombination processes in the gas between the chamber electrodes, especially in the case of UHDR pulsed electron beams (International Atomic Energy Agency 2001, McManus *et al* 2020, Kranzer *et al* 2021, Bourgouin *et al* 2023). Ion recombination processes does not allow to use commercially available ionization chambers for reference dosimetry in FLASH-RT, unless accurate and reliable correction procedures are determined or alternative approaches for gas-based dosimeters are developed (Di Martino *et al* 2022a). On this concern, novel configurations for the ionization chambers are currently under investigation aiming at minimizing the ion recombination within the chamber cavity as the ones reported in Gómez *et al* (2022), Di Martino *et al* (2022b).

A less critical condition in terms of charge recombination in ionization chambers occur for UHDR proton beams, which are mainly accelerated either by isochronous cyclotrons (almost continuous beams) or synchrocyclotrons (pulsed beams), characterized by lower average and instantaneous dose rates (IDRs), respectively with values reaching 200–500 Gy s^{-1} and about 10^4 Gy s^{-1}. In such cases, the ion recombination amount for the commercial ionization chambers, as the PTW Markus and IBA PPC05 chambers can be estimated accurately to correct the chamber signal and measure the dose, as demonstrated in (Darafsheh *et al* 2021, Lee *et al* 2022, Leite *et al* 2023).

However, alternative technologies for reference dosimetry are currently investigated by many research groups to improve the accuracy of the dosimetric procedures for both electron and proton UHDR beams.

Passive dosimeters such as radiochromic films (EBT type) (Jaccard *et al* 2017), alanine pellets (Gondré *et al* 2020), TLD/OSLD (Motta *et al* 2023) already proved to be dose-rate independent, however, like all passive dosimeters they imply offline and time-consuming data analysis, which is not recommended in the perspective of a future clinical translation.

Possible alternative reference dosimeters for FLASH-RT are the portable graphite calorimeters, based on the measurement of the temperature increase of the core during the irradiation. Taking advantage from the almost instantaneous dose delivery at UHDRs, these devices were recently realized with a much less level of technological complexity, making them more suitable for a possible usage in a clinical environment (Bourgouin *et al* 2022, Bass *et al* 2023).

On the other hand, solid state detectors, such as semiconductors and scintillators (sheets and fibers), have certainly shown many advantages, as the high spatial resolution and the fast response (Romano *et al* 2022). Among semiconductors, diamond (Marinelli *et al* 2022), silicon (Medina *et al* 2022, Schönfeld *et al* 2024) and silicon carbide (SiC) (Romano *et al* 2023, Fleta *et al* 2024, Milluzzo *et al* 2024) detectors are currently emerging as promising and reliable dosimeters for FLASH-RT, showing a linear response as a function of the dose per pulse (DPP) and IDRs up to several MGy s^{-1}. Specifically, the flash diamond (fD) dosimeter supplied by the PTW company (2025) is a quite consolidated dosimeter for FLASH-RT and it also allows to perform the dose measurement under the dosimetric reference conditions, i.e. in water (solid or liquid), thanks to its external waterproof and compact holder. On the other hand, silicon and SiC detectors described in Medina *et al* (2022), Milluzzo *et al* (2024) despite demonstrating a good response at the extreme dose rate

of FLASH-RT, are still installed on a typical printed circuit board (PCB), which prevents any measurements in reference conditions, and without secondary charge particle equilibrium. Feta *et al* (2024) describes SiC diodes and the related experimental characterization obtained using the commercial PTW microSilicon housing, enabling measurement under reference conditions (in water). In this contex, in the framework of the INFN CSN5 FRIDA project and the PNRR-PNC ANTHEM project, the first prototype of a homemade encapsulated waterproof SiC detector was recently designed and entirely realized at the INFN Catania division to allow measurements under reference conditions, using the same SiC sensors described in Milluzzo *et al* (2024).

A waterproof version of our SiC detectors (eSiC) would certainly allow punctual dose measurement to be performed in reference conditions, i.e. in water (liquid or solid) and dose distributions measures, such as the percentage dose distribution and the lateral dose profiles, representing a step forward towards the practical use of a SiC dosimeter in a clinical environment.

Absolute and relative dose measurements with both electron and proton UHDR and CONV beams have been performed to prove the reliability of the realized encapsulated SiC (eSiC) prototype for high accuracy FLASH-RT dosimetry.

2. Materials and methods

2.1. SiC detector assembly

SiC detectors, in the typical version installed on a PCB, have been recently produced by the STLab start-up company (STLab srl, (Catania, Italy) 2020) and experimentally tested by the INFN Catania division, as already published in Milluzzo *et al* (2024).

Specifically, a PIN junction is realized with 0.3 μm p+ high doped layer ($N_A = 10^{19}$cm^{-3}) placed on top of a n- low doped layer ($N_D = 8\ 10^{13}$ cm ^{3}) with an active thickness of 10 μm. The two layers are located on top of a $n + 370$ μm thick substrate ($N_D = 5\ 10^{18}$ cm^{-3}). The sensor used for the new encapsulated version of the SiC detector was circular with a total active area of about 4.5 mm^2 and a thickness of 10 μm.

The eSiC, i.e. the capsule as well as any structure to house the SiC detector including the insets for the electrical connections, was designed, realized and embedded at the INFN Catania division within an external PLA waterproof 15 mm diameter 3 cm long cylindrical housing. Specifically, the detector was glued using a conductive paste on top of a customized home-made 3D-printed plastic PCB (figure 1(a)) which was inserted inside an external 1 mm thick cylindrical cup, entirely realized at the INFN Catania Division workshop (figure 1(b)). The internal part of the cylinder was filled with a bicomponent epoxy resin needed to improve the electrical isolation and fill all the internal air gaps. The water equivalent thickness of the layer, i.e. the PLA cup and the small amount of resin in front of the SiC surface was experimentally obtained by comparing the percentage depth dose (PDD) of the 9 MeV UHDR electron beams measured with the eSiC and with measured the fD dosimeter respectively.

As shown in figures 1(a), a 25 μm thick wire bond, realized at the Tecnologie Avanzate Laboratory of the INFN Catania Division, connects the front side of the sensor to the pad used for the charge collection and is connected to the central wire of one of the LEMO cables shown in figure 1(c) for the signal acquisition. The central wire of the second LEMO cable was connected to the back of the sensor to supply the external BIAS voltage (figure 1(a)).

2.2. Experimental campaigns and setups

2.2.1. Measurements with 9 MeV UHDR electron beams

A systematic study of the SiC sensors, mounted on a typical planar PCB (as shown in the inset of figure 1(c)), has been previously performed as reported in Milluzzo *et al* (2024) demonstrating the linear response of such SiC detectors up to an IDR of 5.5 MGy s^{-1}. In this work, we moved from this established configuration to a new setup featuring a cylindrical housing filled with an epoxy resin and including different electrical connections.

As these changes could potentially influence the detector final response, affecting for instance the detector leakage current, we characterized the eSiC detector using the same experimental conditions reported in Milluzzo *et al* (2024), i.e. with the UHDR 9 MeV electron beams accelerated by the ElectronFLASH LINAC (Di Martino *et al* 2020) installed at the Centro Pisano for FLASH Radiotherapy (CPFR) in Pisa (Italy) (Di Martino *et al* 2023), to verify the preserved linear response in the FLASH regime.

The eSiC detector was at first calibrated in dose to water in reference conditions using the customized plastic phantom shown in figure 2(a), at a water depth corresponding to the position of the maximum dose in the depth dose distribution ($\mathbf{D_{max}}$) of the employed 9 MeV electron beams (a 12 mm thick solid water slab was placed) (Di Martino *et al* 2023), using a 10 cm applicator diameter.

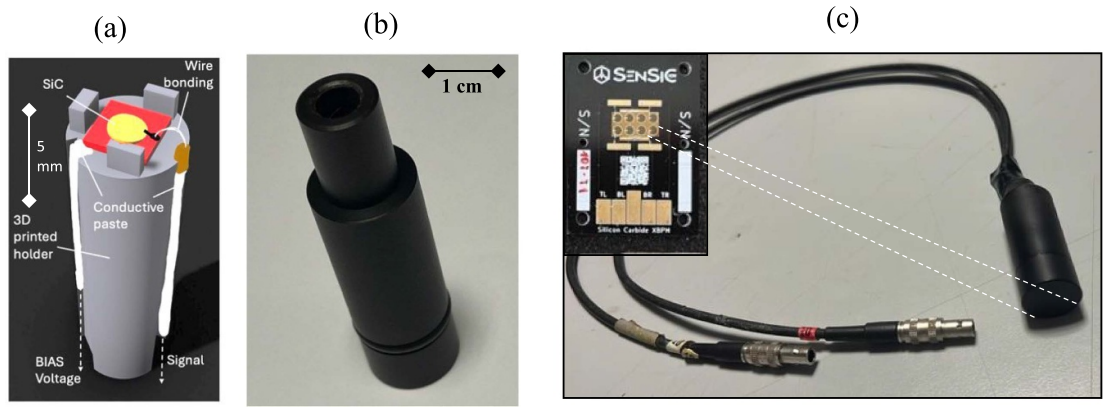

Figure 1. (a) Drawing of the internal structure of the eSiC detector, showing the 3D printed internal cylindrical holder, the wire bonding and the connections. (b) Picture of the external PLA cylindrical holder containing the structure shown in (a). (c) Picture of the final eSiC detector showing the two LEMO cables used to acquire the signal and apply the BIAS voltage. The circular SiC sensor used for the eSiC mounted on a classical PCB is also shown in the inset of (c).

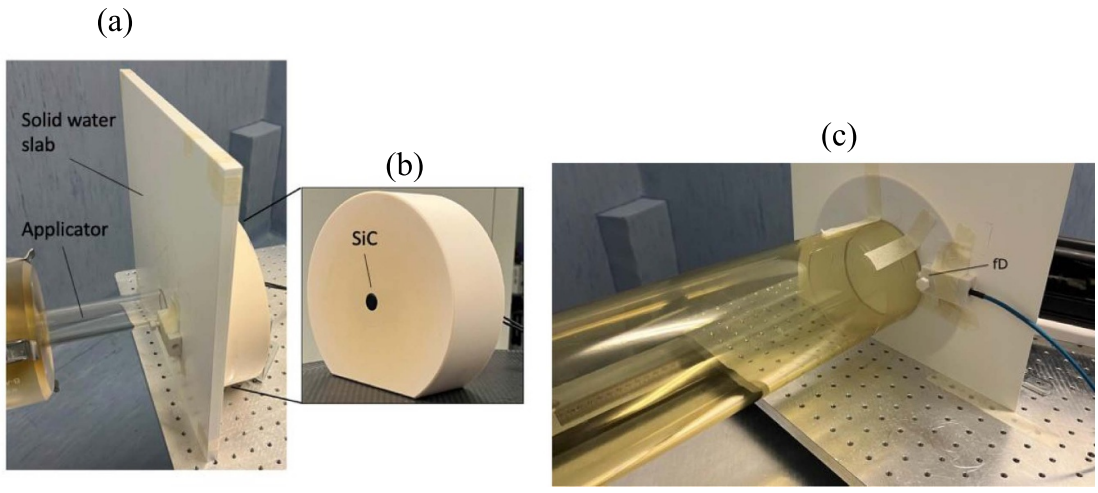

Figure 2. Experimental setup employed at the CPFR showing the applicator and solid water slab (a), the SiC placed in its plastic holder (b), and the setup employed for the PDD measurement with the fD placed off beam.

The external cylindrical shape of the device allowed to use a dedicated phantom to hold it in front of the beam enabling to preserve the lateral secondary charged particle equilibrium (figure 2(b)).

The fD dosimeter already calibrated in dose (3.99 ± 0.10) nc Gy^{-1}) in reference conditions using a CONV clinical LINAC, was used as reference dosimeter during the calibration procedure of the eSiC to provide the absolute dose and obtain a final calibration coefficient for the eSiC of (13.0 ± 0.4) nc Gy^{-1}. The overall uncertainty on the calibration factor is calculated taking into account the statistical uncertainty due to the repetition of the measurements (<1%) and the uncertainty on the calibration factor of the reference dosimeter (3%).

A minimum detectable dose of 2.4 mGy, was calculated for the eSiC dosimeter following the ISO 11 929:2019 standard, which defines the decision threshold and detection limit based on statistical confidence level (95%) and on the measurement uncertainty.

After the calibration, the eSiC response was evaluated at D_{max}, using the 30 mm diameter applicator (figure 2(a)) allowing to span the DPP and, consequently, the IDR, within the single 4 us width pulse, from 1.8 Gy up to 12.4 Gy.

The produced charge within the SiC active layer was acquired using the 6517B Keithley electrometer, which also supplied a BIAS voltage of 80 V to the SiC detector.

The measured charge per pulse was then converted in dose by using the calibration factor in nC Gy^{-1} previously obtained.

The overall uncertainties (uA) on the SiC DPP measurements at different IDR, were determined considering both the type A statistical uA, i.e. the standard deviation of the average dose values obtained

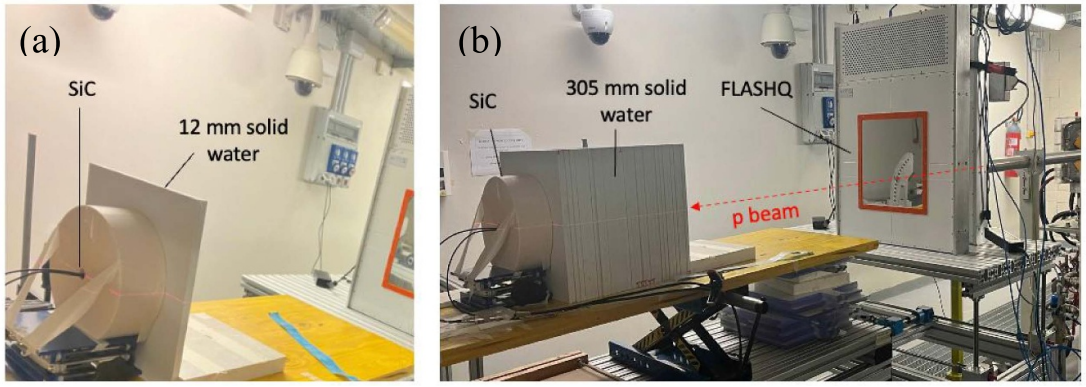

Figure 3. Experimental setup employed with UHDR proton beams with, respectively, 12 mm (a) and 305 mm (b) thick solid water slabs placed in front of the eSiC detector, to get the two different depths in water. The picture also shows the in-transmission monitor ionization chamber.

repeating the measurements under the same condition (5 times) (<1 %) and the type B uA associated with the dose calibration factor (3%). In particular, the final total uncertainty ($u_{tot} = \sqrt{u_A^2 + u_B^2}$), was quoted to be ∼3%.

On the other hand, the measurement of the depth dose distribution was carried out adding different thicknesses of solid water slab in front of the SiC detector from 2 mm up to 46 mm and fixing a DPP of 12.4 Gy and a pulse width of 4 us for these measurements. For each depth, three repetitions were performed to evaluate the average DPP and the corresponding standard deviation (statistical uncertainty). In order to account for the possible pulse-to-pulse beam current fluctuation, the fD detector (2025) was placed off beam beside the SiC detector perpendicular to the beam direction, to intercept the contribution of the secondary particles scattered from the applicator edge that can serve as sort of additional pulse intensity monitor (figure 2(c)). In such way the dose signal measured with the SiC detector was normalized to the one detected simultaneously with the fD detector during each pulse removing any possible dependence on the beam output variability which resulted to be less then 1%.

2.2.2. Measurements with proton beams

A second experimental characterization of the eSiC detector was recently carried out with the proton beams accelerated by the IBA Proteus 235 cyclotron at the Trento Proton Therapy Center.

Specifically, UHDR 228 MeV proton beams and clinical (low dose rate) 180 MeV proton beams were employed.

2.2.2.1. Irradiation with UHDR proton beams

The transport of the 228 MeV proton beams delivered at the experimental research room of the Trento Protonterapy Center (Nuclear Inst 2017), was recently optimized to reach and exceed the average dose rate of 40 Gy/s, therefore allowing for both physical and biological experiments with UHDR proton beams for FLASH RT investigations. The beam current at the exit of the cyclotron can be varied from 1 nA up to 500 nA while the irradiation time can be set using an electronic circuit (generator function) acting on transport elements which can deflect the beam, down to the ms. In order to maintain the linearity of the machine's response, we have kept 10 ms as lower limit for the irradiation time.

The employed setup is shown in figure 3. Before reaching the eSiC detector placed at the isocenter, the proton beams were traversing the in-transmission double gap ionization monitor chamber supplied by the DE.TEC.TOR. company (named FLASHQ) previously calibrated (in terms of MU/Gy) through the IBA reference PPC05 ionization chamber, placed at the same depths of the SiC detector. As reported in Di Martino *et al* (2022b), the low ion recombination occurring in PPC05 chamber with proton beams at these dose rates can be reliably corrected ($k_{sat} = 1.002$).

The eSiC detector was placed at two different water depths: 12 mm and 305 mm corresponding to an energy of the impinging proton beams of about 220 MeV and 40 MeV respectively. Specifically, we used the thicker solid water slab to slightly increase the delivered dose for the same current and irradiation time setting used for the first depth, i.e. placing the detector at a depth closer to the position of the 'Bragg Peak' in the depth dose distribution (Nuclear Inst 2017). The isocenter, fixed at 1.25 m far from the exit window, was in the two cases centered at the surface of the first solid water slab layer. No scattering system able to improve

Table1. Average dose rates measured with the PPC05 chamber at 12 mm and 305 mm water depths corresponding to the different beam current settings.

Beam current (nA)	Average dose rate @ 12 mm (Gy s^{-1})	Average dose rate @ 305 mm (Gy s^{-1})
50	/	55
100	55	111
300	162	331
400	210	425
500	261	527

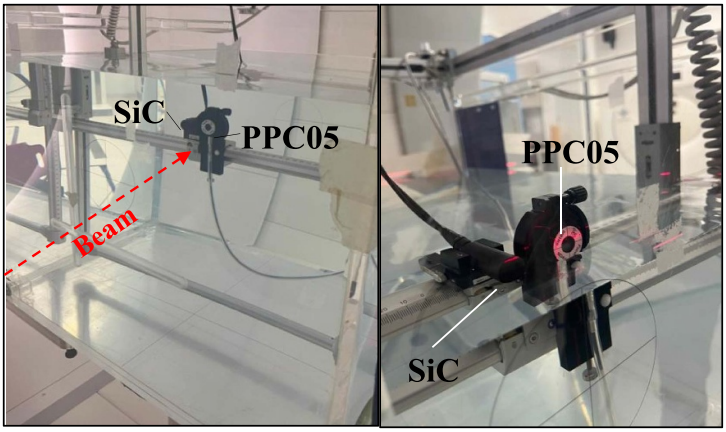

Figure 4. Pictures of the eSiC detector and the PPC05 chamber immersed inside the IBA water phantom during the irradiation with the 180 MeV clinical proton beam performed in one of the two gantries available at the Trento Proton Therapy Center.

the transversal beam homogeneity is employed along the beamline in order to have the maximum achievable dose rate at the isocenter.

However, considering the small area of the exposed SiC detector (2.5 mm diameter) a beam non uniformity correction factor within 3% is expected.

The charge collected within the eSiC detector active layer was acquired with the Keithley 6517B electrometer and then converted in dose using the dose calibration factor. For these measurements no correction was applied accounting for the different qualities of protons and electron beams.

Table 1 reports the values of the average dose rate measured with the PPC05 IBA chamber for the two considered irradiation points and for the different beam current settings. The absorbed dose in water was determined using the calibration factor (N_{DW}) provided in the calibration certificate of the IBA PPC05 chamber and considering the different correction factors (temperature, pressure, ion recombination, etc). An overall uncertainty of 1% is assumed for the PPC05 calibration factor.

2.2.2.2. Irradiation with CONV clinical proton beams

180 MeV clinical pencil beams were used to deliver an homogeneous 10 × 10 cm^2 field in one of the two gantries dedicated to clinical treatments with patients. The eSiC detector and a PPC05 were placed within the IBA motorized water phantom, immersed in water (figure 4) with the beam isocenter set at the center between the two dosimeters. The acquisition of the eSiC detector and the PPC05 was performed simultaneously using a Keithley 6517B electrometer and the IBA DOSE2 electrometer respectively for each step of the motorized phantom along the longitudinal direction. The beam current was monitored during the irradiation by the in-transmission ionization chamber mounted on the gantry head used to normalized both the eSiC and PPC05 chamber signals.

3. Results and discussion

The dose response of the eSiC dosimeter as a function of the DPP measured with the reference fD dosimeter with UHDR electron beams was firstly verified. Figure 5 shows the DPP measured with the eSiC as a function of the reference DPP ranging from 1.8 Gy up to 12.4 Gy per pulse, corresponding to a maximum IDR of 3.1 MGy s^{-1}. A linear fit ($R^2 = 0.99$) was successfully performed as shown in the residuals which reveal a maximum deviation of 1.7%.

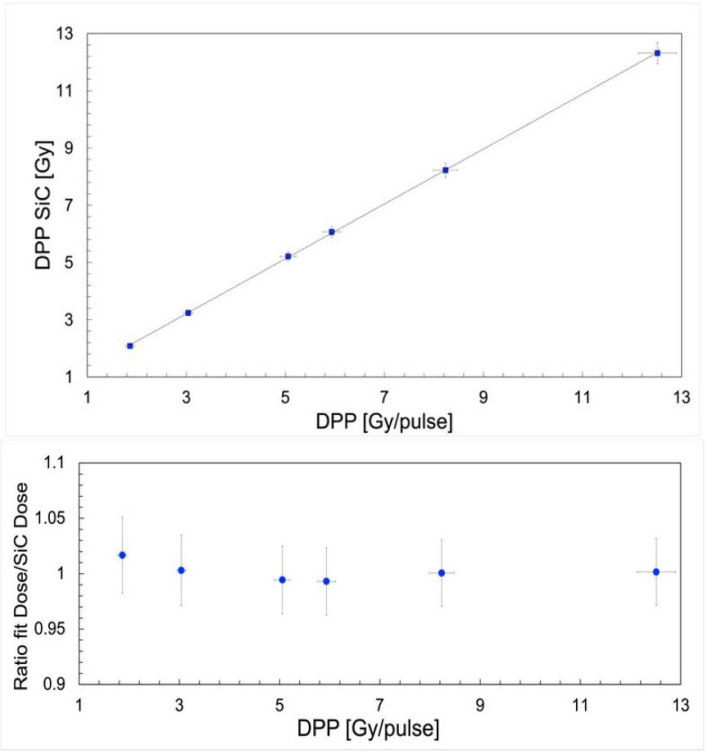

Figure 5. Dose per pulse measured with the eSiC detector as a function of the DPP measured with the fD dosimeter along with the linear fit and the corresponding residuals (bottom).

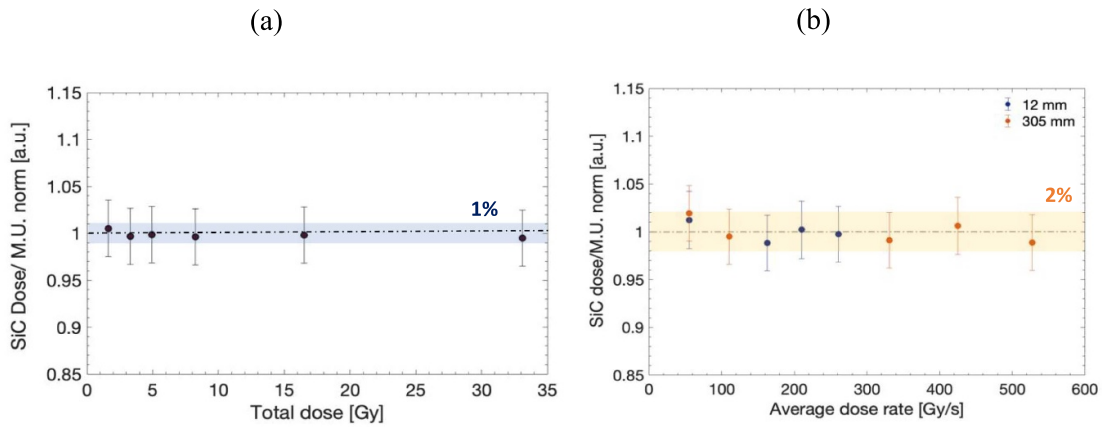

Figure 6. (a) Ratio of the charge measured with the eSiC detector with the UHDR proton beams and the MU detected with the FLASHQ chamber as a function of the total delivered dose for the position at 12 mm water depth (a) and the average dose rate for the two water depths set (b).

To perform a more comprehensive statistical analysis, the data were also fitted with a second-order polynomial to assess which model better described the experimental results. For this purpose, Akaike's information criterion was used, taking into account both the residuals and the complexity of the models. The analysis revealed that the linear model provides the best representation of the experimental data within the investigated DPP range.

The results of the experimental run performed at the Trento Protontherapy facility with the UHDR proton beams are shown in figure 6.

Specifically, figure 6(a) shows the dose measured by the eSiC detector, normalized to the monitor units (MU) simultaneously detected with the in-transmission ionization chamber, as a function of the total delivered dose.

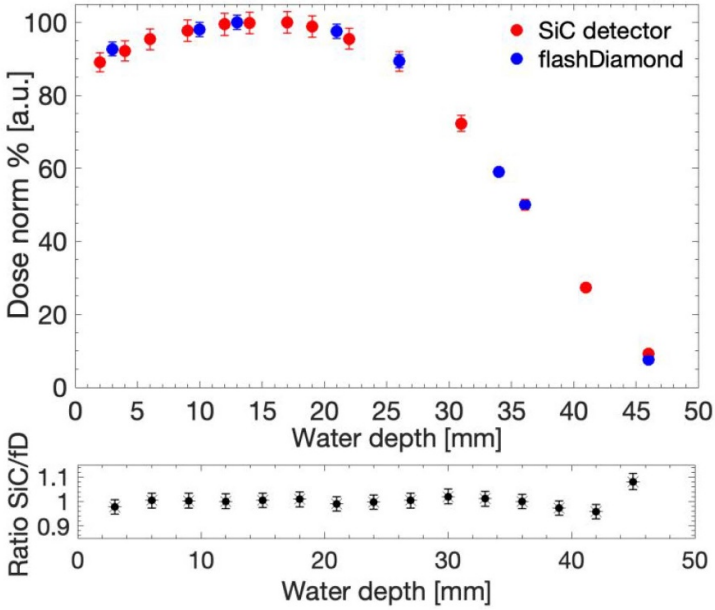

Figure 7. PDD measured with the eSiC detector (red points) and with the fD (blue point) for the 100 mm applicator and a DPP of 12.4 Gy (at the Dmax) obtained using different layer of solid water slabs. The ratio of the normalized signals is also shown in the bottom panel as a function of the water depth.

The average dose rate was kept constant at ∼160 Gy s^{-1}, while the irradiation time was varied between 30 ms and 200 ms to vary the delivered dose. The ratio eSiC dose/MU, normalized to its mean value, remains stable within ±1% across the whole investigated dose range.

To evaluate the possible variation with the average dose rate, the beam current was varied from 50 nA to 500 nA corresponding to the average dose rates reported in table 1 for the two geometrical setups and energies employed. The irradiation time was adjusted to maintain a constant delivered dose of ∼10 Gy. The eSiC signal was then normalized to the MU and five measurements were performed for each condition to determine the mean and the standard deviation of the response (figure 6(b)). Figure 6(b) shows the normalized eSiC dose/MU as a function of the average dose rate. As shown, the detector response remains dose rate independent within ±2% over the tested dose rate range.

The overall uA reported in figures 6 and 7, include the statistical uncertainty arising from the repeated dose measurement in the same conditions (1%–2%) and the dose calibration factor uncertainty for the eSiC (3%).

To prove the reliability of the realized eSiC dosimeter for relative dosimetry measurements, the depth dose distributions of both UHDR electron beams and of the clinical CONV proton beams at the Trento Protontherapy center were measured and compared with reference dosimeters to verify any possible deviation in the measurements.

The PDD of the 9 MeV electron beams measured with the eSiC was compared to the one previously measured with the fD detector. The dose measured at each depth by both the eSiC and the fD were normalized to the D_{max}, to allow the direct comparison. As the water equivalent thickness of the layer in front of the eSiC surface was unknown, the curve measured with the eSiC detector was shifted so that the R_{50} (range at which the dose is the 50% of its maximum) of the two measured PDDs were overlapped. In this way, a water equivalent thickness of the material in front of the eSiC detector of 1.3 mm ± 0.1 mm was indirectly estimated.

As shown in figure 7, a good agreement between the two PDDs is observed, within the measurement uA ($k = 1$). To quantify the discrepancy, the point-by-point ratio between the normalized dose measured with the eSiC and the one obtained by linearly interpolating the fD curve at the same points as the eSiC distribution was calculated (bottom plot of figure 7). The ratio showed a variation within 2% for all depths, confirming an optimal agreement within the uA, except at the 46 mm position, where a 5% discrepancy was observed, mainly attributed to the very low signal at both the eSiC and fD measurements.

The proton depth dose curve was measured employing the 180 MeV clinical proton beam at the Trento Protontherapy Center, performing the measurement directly in liquid water. Figure 8 (top) shows the depth dose distribution simultaneously measured with the eSiC and the PPC05 chamber both normalized to the

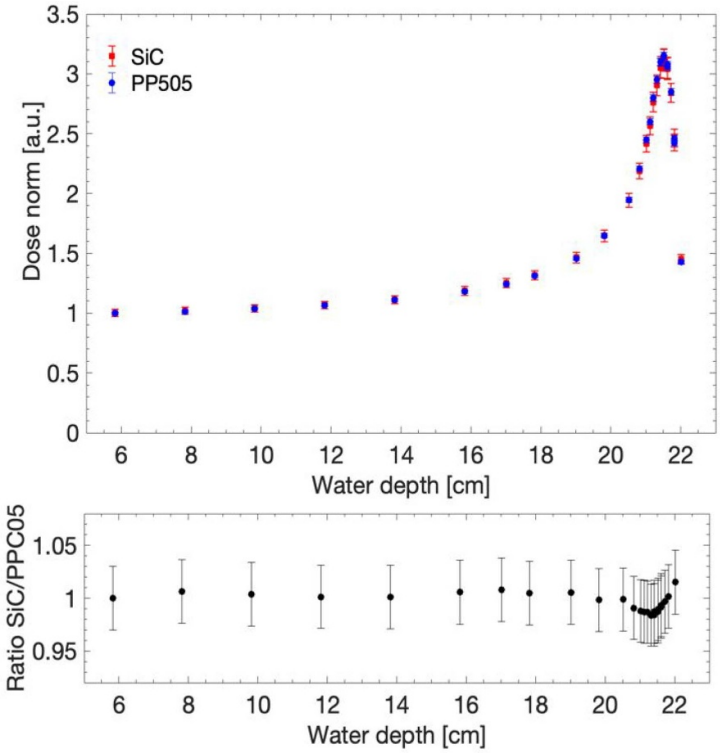

Figure 8. Depth dose distribution of 180 MeV clinical proton beams normalized at the entrance simultaneously measured with the eSiC detector and the IBA PPC05 ionization chamber in water (top). Point-by-point percentage discrepancy between the eSiC and the PPC05 as a function of the water depth (bottom).

MU detected with the in-transmission chamber. Moreover, both the curves were normalized to the measurement at the entrance, i.e. first point of the distribution.

As illustrated in figure 8 (bottom), a discrepancy (in terms of ratio between the two curves) within 1% was observed along the whole proton range demonstrating the capability of the realized eSiC detector to also perform relative dosimetry with high accuracy, certainly comparable with the used reference chamber. A slightly higher discrepancy, still within 2% and, therefore, acceptable for the measurement scope, is observed around the Bragg Peak region which could be ascribed to a possible small dependence of the SiC response from the Linear Energy Transfer in the Bragg peak region. This aspect will be more systematically investigated in the next experimental campaigns.

4. Conclusions

The results reported in this manuscript demonstrate that the first prototype of the eSiC dosimeter, entirely developed at the INFN Catania division, provides accurate dose measurements under both UHDR and CONV electron and proton beams.

We demonstrated that the eSiC dosimeter, where the SiC sensor is embedded within a customized 3D printed waterproof housing, maintains a linear response with the IDR (up to 3 MGy s^{-1}).

Additionally, we tested the eSiC dosimeter with UHDR proton beams for the first time, demonstrating its independence from the total delivered dose and the average dose rate (up to 530 Gy s^{-1}), within $\pm$1% and $\pm$2% respectively. Moreover, the depth-dose curves measured for UHDR 9 MeV electron beams and clinical 180 MeV proton beams showed excellent agreement with the reference dosimeters, namely the fD and the IBA PPC05 chamber respectively, with a variation within 2% across almost the entire particle range.

These promising results lay the basis for the development of standardized and user-friendly SiC-based dosimeters for a future use in clinical applications, including the challenging conditions of FLASH RT. The implementation of a handy SiC dosimeter as described in this work, highlights its capability to perform both reference and relative dosimetry with a high level of accuracy, making SiC technology a reliable, competitive and alternative technology to the already existing solutions, such as the established fD dosimeter, and offering a robust option for future integration into clinical workflows.

Data availability statement

All data that support the findings of this study are included within the article (and any supplementary information files).

Acknowledgment

The presented work was performed within the framework of the national project FLASH Radiotherapy with hIgh Dose-rate particle beAms (FRIDA) and was financed by the National Scientific Committee 5 (CSN5) of the INFN.

This work was also funded by the National Plan for NRRP Complementary Investments (PNC, established with the decree-law 6 May 2021, n. 59, converted by law n. 101 of 2021) in the call for the funding of research initiatives for technologies and innovative trajectories in the health and care sectors (Directorial Decree n. 931 of 06-06-2022)—Project n. PNC0000003—AdvaNced Technologies for Human-centrEd Medicine (Project acronym: ANTHEM). This work reflects only the authors' views and opinions, neither the Ministry for University and Research nor the European Commission can be considered responsible for them.

We also thank Fondazione Pisa for funding CPFR with the Grant prog. n. 134/2021.

We kindly thank the staff of Tecnologie Avanzate service and of the mechanical workshop of the INFN-CT division, namely Nunzio Giudice, Antonio Grimaldi, Francesco Librizzi, Domenico Sciliberto and Antonio Rapicavoli for their valuable support in the preparation of the detectors for the experimental characterization.

Conflict of interest

The authors declare that the research was conducted in the absence of any commercial or financial relationships that could be construed as a potential conflict of interest.

Funding

The authors declare the financial support from the National Scientific Committee 5 (CSN5) of the INFN (FRIDA project) and from the National Plan for NRRP Complementary Investments (ANTHEM Project n. PNC0000003).

ORCID iDs

G Milluzzo 0000-0001-5110-0659
D Zitelli 0009-0005-4157-8380
C Okpuwe 0009-0005-8298-7922
S Lorentini 0000-0003-3202-2581
E Scifoni 0000-0003-1851-5152
F Tommasino 0000-0002-8684-9261
G Trovato 0009-0003-0164-537X
A Quaranta 0000-0003-1320-091X
F Romano 0000-0002-1865-6396

References

Bass G A, Shipley D R, Flynn S F and Thomas R A S 2023 A prototype low-cost secondary standard calorimeter for reference dosimetry with ultra-high pulse dose rates *Br. J. Radiol.* **96** 20220638

Børresen B, Arendt M L, Konradsson E, Bastholm Jensen K, Bäck S Å, Munck Af Rosenschöld P, Ceberg C and Petersson K 2023 Evaluation of single-fraction high dose FLASH radiotherapy in a cohort of canine oral cancer patients *Front. Oncol.* **13** 1256760

Bourgouin A, Keszti F, Schöfeld A A, Hackel T, Kozelka J, Hildreth J, Simon W, Schüller A, Kapsch R-P and Renaud J 2022 The probe-format graphite calorimeter, aerrow, for absolute dosimetry in ultrahigh pulse dose rate electron beams *Med. Phys.* **49** 6635–45

Bourgouin A, Paz-Martín J, Gedik Y C, Frei F, Peier P, Rossomme S, Schönfeld A A, Schüller A, Rodriguez F G and Kapsch R-P 2023 Charge collection efficiency of commercially available parallel-plate ionisation chambers in ultra-high dose-per-pulse electron beams *Phys. Med. Biol.* **68** 235002

Darafsheh A, Hao Y, Zhao X, Zwart T, Wagner M, Evans T, Reynoso F and Zhao T 2021 Spread-out Bragg peak proton FLASH irradiation using a clinical synchrocyclotron: proof of concept and ion chamber characterization *Med. Phys.* **48** 4472–84

Di Martino F *et al* 2020 FLASH radiotherapy with electrons: issues related to the production, monitoring and dosimetric characterization of the beam *Front. Phys.* **8** 570697

Di Martino F *et al* 2022a A new calculation method for the free electron fraction of an ionization chamber in the ultra-high-doseper-pulse regimen *Phys. Med.* **103** 175–80

Di Martino F et al 2022b A new solution for UHDP and UHDR (Flash) measurements: theory and conceptual design of ALLS chamber *Phys. Med.* **102** 9–18
Di Martino F et al 2023 Architecture, flexibility and performance of a special electron linac dedicated to Flash radiotherapy research: electronFlash with a triode gun of the centro pisano flash radiotherapy (CPFR) *Front. Phys.* **11** 1268310
Esplen N, Mendonca M S and Bazalova-Carter M 2020 Physics and biology of ultrahigh dose-rate (FLASH) radiotherapy: a topical review *Phys. Med. Biol.* **65** 23TR03
Favaudon V et al 2014 Ultrahigh dose-rate FLASH irradiation increases the differential response between normal and tumor tissue in mice *Sci. Trans. Med.* **6** 245ra93
Fleta C, Pellegrini G, Godignon P, Rodríguez F G, Paz-Martín J, Kranzer R and Schüller A 2024 State-of-the-art silicon carbide diode dosimeters for ultra-high dose-per-pulse radiation at FLASH radiotherapy *Phys. Med. Biol.* **69** 095013
Gómez F et al 2022 Development of an ultra-thin parallel plate ionization chamber for dosimetry in FLASH radiotherapy *Med. Phys.* **49** 4705–14
Gondré M, Jorge P G, Vozenin M-C, Bourhis J, Bochud F, Bailat C and Moeckli R 2020 Optimization of alanine measurements for fast and accurate dosimetry in FLASH radiation therapy *Radiat. Res.* **194** 573–9
International Atomic Energy Agency 2001 Absorbed dose determination in external beam radiotherapy *Technical Reports Series No.* 398 (IAEA)
Jaccard M, Petersson K, Buchillier T, Germond J-F, Durán M T, Vozenin M-C, Bourhis J, Bochud F O and Bailat C 2017 High dose-per-pulse electron beam dosimetry: usability and dose-rate independence of EBT3 Gafchromic films *Med. Phys.* **44** 725–35
Konradsson E, Arendt M L, Bastholm Jensen K, Børresen B, Hansen A E, Bäck S, Kristensen A T, Munck Af Rosenschöld P, Ceberg C and Petersson K 2021 Establishment and initial experience of clinical FLASH radiotherapy in canine cancer patients *Front. Oncol.* **11** 658004
Kranzer R, Poppinga D, Weidner J, Schüller A, Hackel T, Looe H K and Poppe B 2021 Ion collection efficiency of ionization chambers in ultra-high dose-per-pulse electron beams *Med. Phys.* **48** 819–30
Lee E et al 2022 Ultrahigh dose rate pencil beam scanning proton dosimetry using ion chambers and a calorimeter in support of first in-human FLASH clinical trial *Med. Phys.* **49** 6171–82
Leite A M M, Cavallone M, Ronga M G, Trompier F, Ristic Y, Patriarca A and De Marzi L 2023 Ion recombination correction factors and detector comparison in a very-high dose rate proton scanning beam *Phys. Med.* **106** 102518
Marinelli M et al 2022 Design, realization, and characterization of a novel diamond detector prototype for FLASH radiotherapy dosimetry *Med. Phys.* **49** 1902–10
Mascia A E et al 2023 Proton FLASH radiotherapy for the treatment of symptomatic bone metastases: the FAST-01 nonrandomized trial *JAMA Oncol.* **9** 62–69
McManus M, Romano F, Lee N D, Farabolini W, Gilardi A, Royle G, Palmans H and Subiel A 2020 The challenge of ionization chamber dosimetry in ultra-short pulsed high dose-rate very high energy electron beams *Sci. Rep.* **10** 9089
Medina E, Sangregorio E, Crnjac A, Romano F, Milluzzo G, Vignati A, Jakšic M, Calcagno L and Camarda M 2022 Radiation hardness study of silicon carbide sensors under high temperature proton beam irradiations *Micromachines* **14** 166
Milluzzo G et al 2024 Comprehensive dosimetric characterization of novel silicon carbide detectors with UHDR electron beams for FLASH radiotherapy *Med. Phys.* **51** 6390–401
Moeckli R, Gonçalves Jorge P, Grilj V, Oesterle R, Cherbuin N, Bourhis J, Vozenin M C, Germond J F, Bochud F and Bailat C 2021 Commissioning of an ultra-high dose rate pulsed electron beam medical LINAC for FLASH RT preclinical animal experiments and future clinical human protocols *Med. Phys.* **48** 3134–42
Montay-Gruel P et al 2017 Irradiation in a flash: unique sparing of memory in mice after whole brain irradiation with dose rates above 100 Gy/s *Radiother. Oncol.* **124** 365–9
Montay-Gruel P et al 2021 Hypofractionated FLASH-RT as an effective treatment against glioblastoma that reduces neurocognitive side effects in mice *Clin. Cancer Res.* **27** 775–84
Motta S, Christensen J B, Frei F, Peier P and Yukihara E G 2023 Investigation of TL and OSL detectors in ultra-high dose rate electron beams *Phys. Med. Biol.* **68** 145007
Nuclear Inst 2017 *Methods Phys. Res. A* **869** 15–20
Petersson K, Jaccard M, Germond J-F, Buchillier T, Bochud F, Bourhis J, Vozenin M-C and Bailat C 2017 High dose-per-pulse electron beam dosimetry—A model to correct for the ion recombination in the Advanced Markus ionization chamber *Med. Phys.* **44** 1157–67
PTW 2025 PTW Freiburg GmbH (available at: www.ptwdosimetry.com/en/products/flashdiamond-detector)(Accessed 24 September 2025)
Rohrer Bley C et al 2022 Dose- and volume-limiting late toxicity of FLASH radiotherapy in cats with squamous cell carcinoma of the nasal planum and in mini pigs *Clin. Cancer. Res.* **28** 3814–23
Romano F et al 2023 First characterization of novel silicon carbide detectors with ultra-high dose rate electron beams for FLASH radiotherapy *Appl. Sci.* **13** 2986
Romano F, Bailat C, Jorge P G, Lerch M L F and Darafsheh A 2022 Ultra-high dose rate dosimetry: challenges and opportunities for FLASH radiation therapy *Med. Phys.* **49** 4912–32
Schönfeld A A et al 2024 A 2D detector array for relative dosimetry and beam steering for FLASH radiotherapy with electrons *Med. Phys.* **52** 1845–57
Schulte R et al 2023 Transformative technology for FLASH radiation therapy *Appl. Sci.* **13** 5021
STLab srl, (Catania, Italy) 2020 STLab srl (available at: www.stlab.eu) (Accessed 14 February 2023)
Subiel A, Bourgouin A, Kranzer R, Peier P, Frei F, Gomez F, Knyziak A, Fleta C, Bailat C and Schüller A 2024 Metrology for advanced radiotherapy using particle beams with ultra-high dose rates *Phys. Med. Biol.* **69** 14TR01
Subiel A and Romano F 2023 Recent developments in absolute dosimetry for FLASH radiotherapy *Br. J. Radiol.* **96** 20220560
Velalopoulou A et al 2021 FLASH proton radiotherapy spares normal epithelial and mesenchymal tissues while preserving sarcoma response *Cancer Res.* **81** 4808–21
Vozenin M C et al 2019 The advantage of FLASH radiotherapy confirmed in mini-pig and cat-cancer patients *Clin. Cancer Res.* **25** 35–42
Vozenin M C, Loo B W, Tantawi S, Maxim P G, Spitz D R, Bailat C and Limoli C L 2024 FLASH: new intersection of physics, chemistry, biology, and cancer medicine Rev. *Mod. Phys.* **96** 035002